1

Introduction

1.1 Aeroservoelasticity

Aeroservoelasticity (ASE) is the study of interactions among structural dynamics, unsteady aerodynamics and flight control systems of aircraft (Fig. 1.1), and an active research topic in aerospace engineering. The relevance of ASE to modern airplane design has greatly increased with the advent of flexible, lightweight structures, higher airspeeds and large-bandwidth, automatic flight control systems. The latter trend assumes a greater significance in the modern age, as many of the flight tasks that were earlier performed by a much slower human interface, must now be carried out by high-speed, closed-loop digital controllers, resulting in an increased encroachment into the aeroelastic frequency spectrum. Inadvertent ASE couplings can arise between an automatic flight controller and the aeroelastic modes, resulting in signals becoming unbounded in the closed-loop system. Hence, every new aircraft prototype must be carefully flight-tested to evaluate the ever expanding aeroservoelastic interactions domain, and the higher aeroelastic modes that could be safely neglected in the past must now be fully investigated. Furthermore, favourable ASE interactions can be designed by suitably modifying the feedback control laws, such that certain aeroelastic instabilities are avoided in the operating envelope of the aircraft.

Consider the block representation of the typical ASE system shown in Fig. 1.2. Here, an automatic flight control system is designed to fulfil the pilot commands by actuating control inputs applied to the aircraft. It is seldom possible to model all aspects of an aircraft's dynamics by well-defined mathematical representations. The unmodelled dynamics of the system can be treated as unknown external disturbances applied at various points, such as the atmospheric gust inputs acting on the aircraft and the measurement noise present in the sensors. If such disturbances were absent, one could design an open-loop controller to fulfil all the required tasks. However, the presence of random disturbance inputs necessitates a closed-loop system shown by the feedback loop in Fig. 1.2, where the control inputs are continuously updated based on measured outputs. Such a closed-loop system must be stable and should perform well by following the pilot's commands with alacrity and accuracy. Ensuring the stability and good performance of the closed-loop system in the presence of unknown disturbances is the primary task of the control engineer.

Adaptive Aeroservoelastic Control, First Edition. Ashish Tewari.

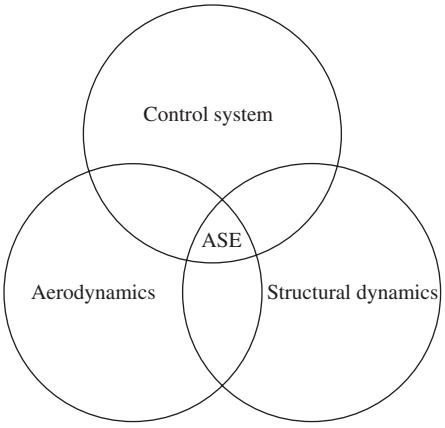

Figure 1.1 Venn diagram showing that aeroservoelasticity (ASE) lies at the intersection of aerodynamics, structural dynamics and flight control systems

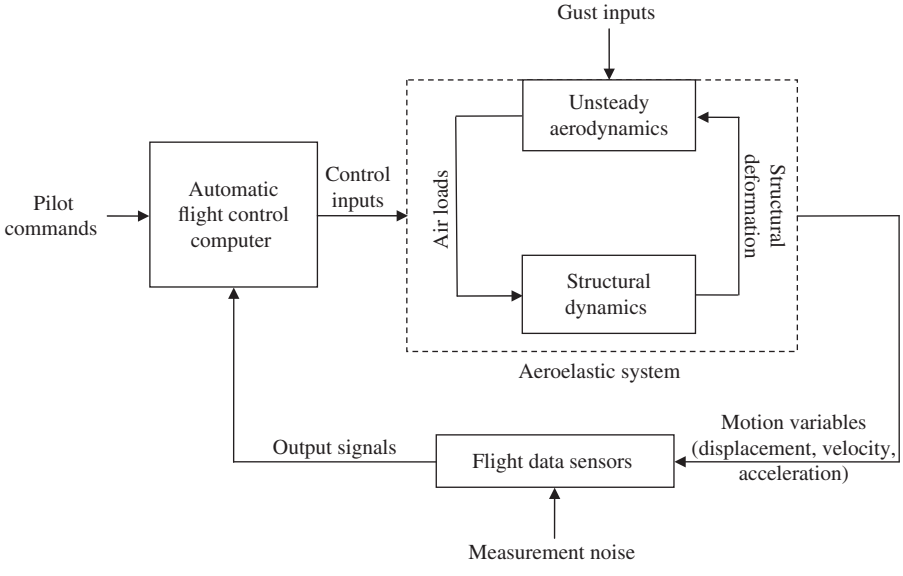

Figure 1.2 Block diagram of a typical flight control system, highlighting the importance of aeroservoelastic analysis

The flight control system is usually designed either without regard to the aeroelastic interactions, or with only the primary, in vacuo structural modes taken into account. When applied to the actual vehicle, such a control system could therefore cause unpredicted consequences due to unmodelled dynamic interaction between the flexible structure and the aerodynamic loads, often leading to instability and structural failure. It is usually left to the flight-test engineers to identify and iron out the problematic ASE coupling of a flying prototype through either a

redesign of the structural members, or reprogramming the flight control computer. This process is time consuming, expensive and very often fraught with danger. However, if the ASE analysis is introduced as a systematic procedure into the basic airframe and flight control design from the conceptual stage, such difficulties can be avoided at a more advanced stage. The focus of the present book is to devise such a systematic procedure in the form of an adaptive design of the flight control system.

The most important ASE topic is the catastrophic phenomenon of flutter, which is an unstable dynamic coupling between the elastic motion of the wings (or tails) and the unsteady aerodynamic loading that generally begins at a small amplitude, and grows to large amplitudes thereby causing structural failure. The classical flutter mechanism consists of an interaction between two (or more) natural aeroelastic modes at a critical dynamic pressure, and can be excited by either atmospheric gusts or control surface movement. While traditional method of avoiding flutter consists of stiffening the structure such that the natural modes causing flutter occur outside the normal operating envelope of the aircraft, such a method is not always reliable, and requires many design iterations based on expensive, cumbersome and dangerous flight-tests of actual prototypes. The main problem lies in accurately predicting the critical dynamic pressure, because of a drastic change in aerodynamic characteristics due to Mach number and the equilibrium angle of attack. Such a bifurcation typically occurs at transonic speeds and requires a nonlinear stability analysis. For example, the flutter dynamic pressure computed by linearized subsonic aerodynamics is often much higher than that actually encountered at transonic Mach numbers. Since the non-conservative dip in the flutter dynamic pressure due to transonic effects can be extremely treacherous, either accurate computational fluid dynamics (CFD) modelling or precise wind-tunnel experiments are necessary for predicting transonic flutter modes. However, both CFD modelling and wind-tunnel testing are complicated by the sensitivity of nonlinear transonic aerodynamics to transition and turbulence, for which no CFD model or experimental technique, however advanced, can be entirely relied upon. Even an extremely sophisticated Navier–Stokes computation with tens of million of grid points is unable to resolve the fine turbulence scales of an unsteady transonic flowfield on a complete aircraft configuration. Furthermore, these same aeroelastic phenomena have large-scale effects (Edwards 2008), which make an extrapolation of wind-tunnel data to the full-scale aircraft highly uncertain. The inadequacies of aerodynamic modelling can be practically overcome only by an adaptive, closed-loop identification and control of unsteady aerodynamics, which is the topic of the present book.

Actively suppressing flutter through a feedback control system is an attractive alternative to passive flutter avoidance by haphazard redesign and flight testing. The concept of active flutter suppression began to be explored in the 1970s (Abel 1979), wherein an automatic control system actuated a control surface on the wing, in response to the structural motion sensed by an accelerometer. This modified the aeroelastic coupling between critical modes, such that the closed-loop flutter occurred at a higher dynamic pressure. Linear feedback control design for active flutter suppression requires an accurate knowledge of the aeroelastic modes that cause flutter. Although the classical flutter of a high aspect-ratio wing of a transport type aircraft is caused by an interaction between the primary bending and torsion aeroelastic modes, the flutter mechanism of a low aspect-ratio wing of a fighter-type airplane involves a coupling of several aeroelastic modes. Despite extensive research (Abel and Noll 1988, Perry *et al*. 1995), active flutter suppression has yet to reach operational status. This shortcoming is due to the inability of designing a feedback control system that can be considered sufficiently robust with respect to

the parametric uncertainties caused by nonlinear transonic effects which, as mentioned earlier, are difficult to predict. Routine implementation of active flutter suppression must wait until suitably accurate transonic ASE design methods are available. Hence, development of practical adaptive control techniques for transonic flutter suppression will be a revolutionary step in the design of automatic flight control systems.

The process of adaptive aeroservoelastic design is briefly introduced in this chapter, although full explanations will follow in the subsequent chapters. ASE applications require designing an underlying feedback control system (Chapter 2) in order to ensure closed-loop stability in a range of operating conditions. Such a design is typically based upon a linearized model of the underlying aeroelastic system, which is discussed in Chapter 3. The aircraft has a continuous structure, but for computational considerations it is approximated by finite degrees of freedom using a process such as the finite element method (FEM). In a complete wing–fuselage–tail combination, this approximation may require several thousand degrees of freedom for an accurate representation. However, as most aeroelastic phenomena of interest involve only about a dozen structural modes, the structural displacement vector $\{z(t)\}$ [1] can be represented as a linear combination of a few structural vibration modes given by the vector of modal degrees of freedom $\{q(t)\}$ (also called the generalized coordinates), and result in the following generalized equations of motion:

$$[M]\{\ddot{q}\} + [C_d]\{\dot{q}\} + [K]\{q\} = \{Q\}(\{q\}, \{\dot{q}\}, \{\ddot{q}\}), \tag{1.1}$$

where $[M], [C_d], [K]$ are the generalized mass, damping and stiffness matrices representing the individual masses, viscous damping factors and moments of inertia corresponding to the various modal degrees of freedom, and $\{Q(t)\}$ is the generalized aerodynamic force vector, whose dependence upon the modal degrees of freedom (and their time derivatives) requires separate modelling.

1.2 Unsteady Aerodynamics

The computation of unsteady aerodynamic forces $\{Q(t)\}$ from structural degrees of freedom is the main problem in aeroelastic modelling. The fluid dynamics principles upon which such an aerodynamic model is based require a conservation of mass, momentum and energy of fluid flowing through a control volume surrounding the aircraft. As in the case of the structural model, a CFD model necessitates the approximation of the continuous fluid flow by a finite number of cells (called a grid), within each of which the conservation laws can be applied, and then summed over the entire flowfield. The grid can either have a well-defined shape (called structured grid) or could be entirely unstructured in order to give flexibility in accurately modelling the moving, solid boundary. The spatial summation from individual grid points to the entire flowfield can be carried out by finite difference, finite volume or finite element methods, each requiring a definite discretization process. There is also the possibility of using simplifying assumptions in applying the conservation laws. For example, the airflow about a wing $(x, y) \in S, z_\ell \le z \le z_u$ at a sufficiently large Reynolds number can be regarded to be largely inviscid, with the viscous effects confined to a thin region close to the wing (boundary layer) and in its wake. This affords a major simplification, wherein $\{Q(t)\}$ is computed from

[1] Vectors and matrices in this chapter are denoted by braces and brackets, respectively. A more compact notation follows in the next chapter.

continuity, inviscid momentum and energy conservation (Euler equations) applied outside the boundary layer and wake, and integrated in space (x, y, z) subject to suitable unsteady boundary conditions. These latter include the solid boundary condition of no flow across the moving wing surface, and tangential velocity continuity at its trailing edge (the Kutta condition) due to the presence of viscosity in the boundary layer and wake.

The unsteady Euler equations can be written in the conservation form as follows:

$$\frac{\partial\{F\}}{\partial t} + \frac{\partial\{f_x\}}{\partial x} + \frac{\partial\{f_y\}}{\partial y} + \frac{\partial\{f_z\}}{\partial z} = \{0\}, \tag{1.2}$$

where

$$\{F\} = \{\rho, \rho u, \rho v, \rho w, \rho e\}, \tag{1.3}$$

is the independent flow variables vector, with ρ being the density, e the specific internal energy,

$$\{V\} = \{u, v, w\}, \tag{1.4}$$

the velocity vector with (u, v, w) being the velocity components along (x, y, z), respectively, and

$$\begin{aligned} \{f_x\} &= u\{F\} + \{0, p, 0, 0, pu\} \\ \{f_y\} &= v\{F\} + \{0, 0, p, 0, pv\} \\ \{f_z\} &= w\{F\} + \{0, 0, 0, p, pw\}, \end{aligned} \tag{1.5}$$

are the flux vectors along x, y and z directions, respectively. The flux gradients, $\frac{\partial f_x}{\partial x}$, $\frac{\partial f_y}{\partial y}$, $\frac{\partial f_z}{\partial z}$, are required to be modelled differently according to the local direction of the infinitesimal pressure waves. Clearly, even the Euler equations are inherently nonlinear, requiring an iterative solution procedure, which is further complicated by having to model an entropy condition for a unique solution, usually by introducing artificial viscosity into the solution procedure. An artificial viscosity model can lead to spurious frequency spectra in unsteady flow computations. Alternatively, a solution by flux direction biasing or splitting algorithms in finite-element (or finite-volume) methods is employed, which can have further problems of non-physical oscillations when the sonic condition is encountered in the flowfield. Dealing with non-unique and physical solutions is a major problem associated with Euler equations, often requiring sophisticated computational procedures that add to the computational time.

An additional approximation is invariably necessary for modelling purposes, namely that of potential flow with small perturbations. However, even the full-potential (FP) and small-disturbance solutions for the transonic regime are inherently nonlinear and iterative and fraught with non-unicity and non-physical nature, such as the prediction of expansion shock waves. As in the case of Euler solvers, the closure of the inviscid, potential computational problem necessitates the addition of an entropy condition in the form of either artificial viscosity or flux biasing/splitting. Consequently, little is gained in terms of computational complexity by making the potential approximation of unsteady transonic flows. Owing to their iterative nature and high computational times, the unsteady CFD computations of nonlinear governing equations are infeasible to carry out in a real time adaptive control scheme, which may require several evaluations of $\{Q(t)\}$ per time step. Only in the subsonic and supersonic regimes can the small-disturbance potential equation be linearized. In such a

case, the unsteady aerodynamic computation involves an integration of pressure distribution $p(x, y, z, t)$ on the wing surfaces, subject to the flow velocity normal to the wing (normalwash) $\{V\} \cdot \{n\}$ created by the structural vibration modes. If the wing is thin ($z_\ell \simeq z_u$), the vibration amplitudes are small, and there are no aerodynamic dissipation mechanisms present (such as viscous flow separation and shock waves), the pressure–normalwash relationship is rendered linear, and is given by the following integral equation:

$$w(x, y, t) = \int_S K[(x, y : \xi, \eta), t] \Delta p(\xi, \eta, t) \mathrm{d}\xi \mathrm{d}\eta, \tag{1.6}$$

where $\Delta p = p_\ell - p_u$ is the pressure difference between the lower and upper faces of the essentially flat wing's mean surface at a given point (ξ, η), and $w(x, y, t)$ the flow component normal to the mean surface (z-component) called the upwash (or its opposite in sign, the downwash). Such a simple relationship is enabled by the process of linear superposition of elementary, flat plate (or panel) solutions to the governing partial differential equation. However, while Eq. (1.6) can be applied in subsonic and supersonic flows about thin wings with small vibrations, it is invalid in the transonic regime, where nearly normal shock waves are always present and cause viscous separation in the boundary layer and wake. Furthermore, even in subsonic and supersonic regimes, the linear superposition cannot be applied around thick wings undergoing large amplitude vibration, as flow separation or strong shock waves could be present.

A linear aerodynamic model Eq. (1.6) combined with the linear structural dynamics Eq. (1.1) yields the following linear aeroelastic state equations that can be used as a baseline plant of the adaptive ASE control system:

$$\{\dot{X}\} = [A]\{X\} + [B]\{u\} + [F]\{p\}, \tag{1.7}$$

where $\{X(t)\} = [\{q(t)\}^T, \{\dot{q}(t)\}^T]^T$ is the state vector of the aeroelastic system, $\{u(t)\}$ the vector of generalized control forces generated by a set of control surfaces and $\{p\}$ the vector of random disturbances called the process noise. In order to derive the constant coefficient matrices $[A], [B], [F]$, an additional step is necessary, even if the generalized aerodynamic forces $\{Q(t)\}$ are linearly related as follows to the modal displacements $\{q(t)\}$ and their time derivatives by virtue of Eq. (1.6):

$$\{Q(s)\} = [G(s)]\{q(s)\}, \tag{1.8}$$

where s is the Laplace operator and $[G(s)]$ denotes the unsteady aerodynamics transfer matrix. The essential step is modelling of $[G(s)]$ by a suitable rational-function approximation (RFA), such as the following:

$$[G(s)] = [A_0] + [A_1]s + [A_2]s^2 + \sum_{j=1}^{N} [A_{j+2}] \frac{s}{s + b_j}, \tag{1.9}$$

where the numerator coefficient matrices, $[A_0], [A_1] + [A_2], [A_{j+2}], j = 1, \cdots, N$ are determined by curve fitting $[G(i\omega)]$ to the simple harmonic aerodynamics data ($s = i\omega$) at a discrete set of frequencies ω, and for each flight condition (speed and altitude). Additionally,

the denominator coefficients $b_j, j = 1, \cdots, N$ may be selected by a nonlinear optimization process, whereby the curve fit error in a range of frequencies is minimized. Such an optimized curve fitting is not a trivial matter, and is by itself an area of major research with the objective of deriving an accurate RFA, which is also of the minimum possible order. The order of the state space model (the dimensions of $[A]$) increases rapidly with the order of the RFA, and the computational effort in optimizing the denominator coefficients could be significant especially if a large range of flight conditions is involved. For this reason, several different RFA techniques have been proposed in the literature. However, in keeping with the present objective of designing an adaptive control system, RFA optimization must be carried out offline and its results stored in order to derive the baseline aeroelastic plant model in the flight conditions of interest. The frequency domain (simple harmonic) data to be used for RFA derivation is also pre-computed by a suitable linearized small-disturbance, potential aerodynamic model, such as that based on the integral equation, Eq. (1.6). After the RFA for the aerodynamic transfer-matrix, Eq. (1.9), is derived, a linear, time-invariant, state-space model, Eq. (1.7), for the aeroelastic system – perhaps also including the control-surface actuators model – is obtained.

1.3 Linear Feedback Design

Consider the basic automatic control system shown in Fig. 1.3, where the automatic controller is designed as a generic device to exercise control over the plant, in order that the entire control system meets a certain set of desired objectives, and follows a desired trajectory, $\{x_d(t)\}$. For the purposes of this book, the desired trajectory is taken to be a constant equilibrium state, $\{x_d(t)\} = \{0\}$, wherein the control strategy to be evolved becomes a regulator problem. If the plant can be described precisely by a set of fixed mathematical relationships between the input, $\{u(t)\}$, and output, $\{y(t)\}$, variables, then the controller can usually be designed fairly easily in order to meet the performance requirements in a narrow range of operating conditions (Tewari 2002). Such a controller would have a fixed structure (often linear) and constant parameters. However, a physical plant almost never conforms exactly to any deterministic mathematical description due to either improperly understood physical laws, or unpredictable external disturbances treated as stochastic signals (the process noise vector), which is shown in Fig. 1.3 as the externally applied random vector signal, $\{p(t)\}$.

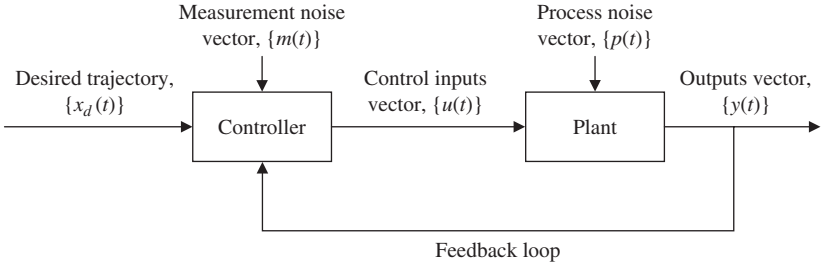

Figure 1.3 Basic automatic control system with a feedback control loop

Similarly, the controller, when physically implemented, has its own imperfections that defy precise mathematical description. For the feedback controller, such a departure from a deterministic controller model is shown as the measurement noise vector, $\{m(t)\}$, appearing in the feedback loop. The success of the automatic controller in performing its task of tracking the reference signals with any accuracy depends upon how sensitive the control system is to the unmodelled noise signals, $\{p(t)\}, \{m(t)\}$. If no regard is given to the noise signals while designing the controller, there is a real possibility that the control system will either break down completely, or have a poor performance when actually implemented. The controller design is therefore carried out to ensure adequate robustness with respect to the noise signals. A feedback loop by itself provides a certain degree of robustness with respect to unmodelled process and measurement noise. If the feedback control parameters are suitably adjusted (fine-tuned), the sensitivity to noise inputs can be further reduced. Such a design is called loop shaping (Chapter 2). For a plant with a linear input–output behaviour and a fair statistical description of the noise inputs that are small in magnitude, the robust control theory (Maciejowski 1989) can be applied to design a linear feedback controller with constant parameters, which will produce an acceptable performance in many applications. However, constant controller gains may either fail to stabilize the system if the plant behaviour is highly uncertain or may have unacceptable performance in the presence of noise inputs. In such cases, the alternative strategy of sensing the actual plant behaviour and to adapt the controller gains to suit a certain minimum performance level in a range of operating conditions is the only answer. Such a strategy where the controller parameters are functions of the sensed plant state vector is called adaptive control, and is nonlinear by definition. In summary, design of an automatic controller can be alternatively based on ensuring a high level of robustness with respect to unmodelled dynamics with constant controller parameters by a design process called robust control or by making the controller parameters adapt to a changing plant behaviour through an adaptation mechanism. The two design techniques of robust control and adaptive control may appear to be contradictory in nature, because in one case the controller is deliberately made impervious to process and measurement noise, while in the other, the controller is asked to change itself with a changing plant dynamics. However, if a compromise can be carried out in the two methods of synthesis, the result can be a synergistic fusion of robust and adaptive control. In such a case, the high-frequency noise (which is typically of small magnitude) is sought to be rejected by an inbuilt control robustness, while the much slower but larger amplitude variations in the plant dynamics are sensed and carefully adapted to. Such an ideal combination of robustness and adaptation is the goal of most control system designers.

An important step in ASE design is to derive a baseline multivariable feedback controller for active stabilization by standard linear closed-loop techniques, such as eigenstructure assignment and linear optimal control (Tewari 2002). For example, if a linear optimal regulator is sought, one minimizes the following quadratic Hamiltonian function with respect to the control variables, $\{u(t)\}$, subject to linear dynamic constraint of Eq. (1.7):

$$H = \frac{1}{2}\{X\}^T[Q]\{X\} + \{X\}^T[S]\{u\} + \frac{1}{2}\{u\}^T[R]\{u\} + \{\lambda\}^T([A]\{X\} + [B]\{u\}), \qquad (1.10)$$

where $[Q], [S], [R]$ are the constant, symmetric cost coefficient matrices, and $\{\lambda(t)\}$ is the vector of co-state variables. The necessary conditions for optimality with an infinite control

interval are then given by the following Euler–Lagrange equations:

$$\{\dot{\lambda}\} = -\left(\frac{\partial H}{\partial \{X\}}\right)^T = -[Q]\{X\} - [S]\{u\} - [A]^T\{\lambda\}, \tag{1.11}$$

$$\{\lambda\}(\infty) = \{0\}, \tag{1.12}$$

$$\frac{\partial H}{\partial \{u\}} = \{0\} = [S]^T\{X\} + [R]\{u\} + [B]^T\{\lambda\}, \tag{1.13}$$

the last of which is solved for the optimal control vector to yield the following:

$$\{u\} = -[R]^{-1}\left([S]^T\{X\} + [B]^T\{\lambda\}\right). \tag{1.14}$$

Substitution of Eq. (1.14) into Eqs. (1.7) and (1.11) results in the following set of linear state and co-state equations:

$$\{\dot{X}\} = \left([A] - [B][R]^{-1}[S]^T\right)\{X\} - [B][R]^{-1}[B]^T\{\lambda\}, \tag{1.15}$$

$$\{\dot{\lambda}\} = -\left([A]^T - [S][R]^{-1}[B]^T\right)\{\lambda\} + \left([S][R]^{-1}[S]^T - [Q]\right)\{X\}, \tag{1.16}$$

which have to be solved subject to the following two-point boundary conditions,

$$\{X\}(0) = \{X_0\}; \quad \{\lambda\}(\infty) = \{0\}. \tag{1.17}$$

The simultaneous forward and backward time-marching required for the solution of Eqs. (1.15) and (1.16) is commonly expressed as the following linear feedback control law with a constant gain matrix, $[K]$:

$$\{u\} = -[K]\{X\}, \tag{1.18}$$

where

$$[K] = [R]^{-1}\left([B]^T[P] + [S]^T\right), \tag{1.19}$$

and the constant matrix $[P]$ is the solution to the following algebraic Riccati equation (ARE):

$$\begin{aligned}\{0\} = [Q] + \left([A] - [B][R]^{-1}[S]^T\right)^T[P] + [P]\left([A] - [B][R]^{-1}[S]^T\right)\\ -[P][B][R]^{-1}[B]^T[P] - [S][R]^{-1}[S]^T.\end{aligned} \tag{1.20}$$

The ARE is a nonlinear algebraic equation and necessitates an iterative solution procedure, which must be carried out for each set of coefficient matrices $[A], [B], [Q], [R], [S]$. This is, in a nutshell, the linear, quadratic regulator (LQR) problem with a quadratic cost and an infinite control horizon. The cost coefficients $[Q], [R], [S]$ must be selected such that the regulator is an asymptotically stable system, which requires that all the eigenvalues of the closed-loop dynamics matrix, $[A] - [B][K]$, should lie in the left-half side of the Laplace domain. Alternatively, the eigenvalues and eigenvectors of the dynamics matrix, $[A] - [B][K]$, can be directly specified in order to determine $[K]$, which is termed an eigenstructure assignment.

The state feedback regulator cannot be directly implemented because the state variables of the aeroelastic plant, $\{X\}$, are unavailable for direct measurement. What one can measure are

the output variables, $\{y\}$, detected by a set of sensors placed strategically on the aircraft. The state vector, $\{X\}$, which is required by the linear feedback control law, Eq. (1.18), must then be constructed by an additional system called an observer (or state estimator). The linear output equation,

$$\{y\} = [C]\{X\} + [D]\{u\} + \{m\}, \tag{1.21}$$

where $\{m(t)\}$ is the vector of random disturbances (the measurement noise), can be used to design a full-order observer, whose dynamics is governed by the following state equation:

$$\{\dot{\hat{X}}\} = ([A] - [L][C])\{\hat{X}\} + ([B] - [L][D])\{u\} + [L]\{y\}, \tag{1.22}$$

where $\{\hat{X}\}$ is the estimated state vector, and $[L]$, the observer gain matrix. Such an observer requires that the plant must be observable with the outputs given by Eq. (1.21). The observer gain matrix, $[L]$, can be selected in a manner similar to (but separately from) the regulator gain, $[K]$, by either eigenstructure assignment for the observer dynamics matrix, $[A] - [L][C]$, or via linear, quadratic, optimal control where $[A]$ is replaced by $[A]^T$, and $[B]$ by $[C]^T$. The optimal observer is also known as the Kalman filter and is guaranteed to minimize the covariance matrix, $[R_e]$, of the estimation error, $\{e\} = \{X\} - \{\hat{X}\}$, in the presence of zero-mean, Gaussian process and measurement noise signals, $\{p\}$, $\{m\}$. In the infinite horizon case, the Kalman filter gain is determined by the following ARE similar to Eq. (1.20), and hence the Kalman filter is regarded as the dual of the state feedback regulator.

$$\begin{aligned}\{0\} = {} & [A_G][R_e] + [R_e][A_G]^T - [R_e][C]^T[S_m]^{-1}[C][R_e] \\ & + [F]\left([S_p] - [S_{pm}][S_m]^{-1}[S_{pm}]^T\right)[F]^T,\end{aligned} \tag{1.23}$$

where $[S_m], [S_p], [S_{pm}]$ are the matrices of power spectral density of the measurement noise, $\{m\}$, that of the process noise, $\{p\}$, and the cross-spectral density of $\{p\}, \{m\}$, respectively, and

$$[A_G] = [A] - [F][S_{pm}][S_m]^{-1}[C]. \tag{1.24}$$

The Kalman filter gain matrix is then given by

$$[L] = \left([R_e][C]^T + [F][S_{pm}]\right)[S_m]^{-1}. \tag{1.25}$$

Clearly, the matrices $[S_m], [S_p], [S_{pm}]$ act as the cost coefficients of a quadratic objective function for determining $[L]$ in a manner similar to $[Q], [R], [S]$ for the LQR regulator. These should be suitably selected in the observer design process.

The observer's dynamics must be designed to be stable and much faster than the regulator. It is crucial for practical considerations that the derived control laws must be robust with respect to modelling uncertainties (process noise) and sensor (measurement) noise at a selected range of operating conditions. The procedure by which an LQR and a Kalman filter (also called linear, quadratic estimator (LQE)) are designed separately for a linear, time-invariant plant, and then put together to form a compensator is referred to as the linear, quadratic, Gaussian (LQG) method. Here, the Kalman filter supplies the estimated state for feedback to the LQR regulator. The design of the LQG compensator – specified by the gain matrices, $[K], [L]$ – depends upon the chosen cost parameters, $[Q], [R], [S], [S_m], [S_p], [S_{pm}]$. Suitable performance and robustness requirements of the overall ASE system restrict the choice of the cost parameters to a specific range. Being based upon optimal control, an LQG compensator has excellent performance

features for a given set of cost parameters, but its robustness depends upon how much the performance is degraded by state estimation through the Kalman filter. If the observer gains, $[L]$, are too small, the estimation error, $\{e\}$, does not tend to zero fast enough for the feedback to be accurate. On the other hand, if the observer has very large gains, there is an amplification of process and measurement noise by feedback, thereby reducing the overall robustness of the control system. Clearly, a balance must be struck in selecting the Kalman filter design parameters, such that a good robustness is obtained without unduly sacrificing performance. Several linear feedback strategies are in use for striking a compromise between robustness with respect to plant uncertainty, and noise rejection properties. These include LQG compensation with loop-transfer recovery (LTR) (Maciejowski 1989), H_2/H_∞ control (Glover and Doyle 1988) and structured singular value (SSV) (or μ-) synthesis (Packard and Doyle 1992). Chapter 2 is a brief compilation of the basic linear feedback design methods for achieving a robust control system with constant parameters.

1.4 Parametric Uncertainty and Variation

Any aeroelastic model employed in ASE design is likely to have modelling uncertainties in its parameters, $[A], [B], [C], [D]$. These can be either due to errors in the linear aeroelastic plant or due to a part of the dynamics which is entirely unmodelled. The parametric errors in the linear plant are due to inadequacies of the structural dynamics model, as well as those in evaluating the frequency domain aerodynamics and its transfer matrix (RFA) representation. The unmodelled dynamics include nonlinear structural and aerodynamic effects, which are difficult to account for. While linear parametric uncertainties are easier to handle in a control system design, it is the presence of unmodelled dynamics that causes a greater anxiety. Of these, the nonlinear aerodynamic phenomena are the most critical as they can cause unforeseen aeroelastic instabilities, and whose model requires iterative and complex CFD computations which (as noted above) are infeasible to carry out in real time. Aerodynamic nonlinearities encountered in aeroservoelastic systems are divided into two classes: (i) unsteady behaviour involving normal shock waves and (ii) largely separated or vortex-dominated flows. While type (i) is only present at the transonic speeds, nonlinearities of type (ii) occur at high angle-of-attack flight. A fighter-type aircraft manoeuvring at transonic speeds will encounter both the effects. The unsteady flow separation (type (ii)) causes a buffeting of the airframe at low frequencies, and can result in rigid dynamic instabilities, such as wing-rock, nose-slice and coning motions, but rarely cause an aeroelastic coupling. This is due to the fact that the structural dynamics of the airframe simply acts as a stable, linear filter of the nonlinear buffeting forces and moments, allowing the peaks of the spectrum to occur only at the in vacuo structural frequencies. Consequently, notch-filters can be designed to suppress the buffet at well-identified frequencies. Such a nonlinear dynamic characteristic can be analysed by the Popov stability criterion (Chapter 7). However, the shock-wave effects (type (i)) are more interesting; they cause dynamic aeroelastic instabilities, leading to a sharp reduction in the flutter dynamic pressure and a sustained limit-cycle oscillation (LCO), often ending in a catastrophic structural failure. An accurate transonic aerodynamic model is necessary to account for unsteady shock wave effects and an absence of such a model renders the unsteady aerodynamic forces and moments highly uncertain.

In addition to modelling uncertainties, there are significant variations in the aeroelastic characteristics due to changing operating conditions (flight speed and altitude). For example, as the

flight Mach number is increased from subsonic to supersonic, the variation of the lift, pitching moment and control-surface hinge moment with angle-of-attack and control deflections vary drastically. Some steady-state aerodynamic derivatives can even change in sign as the transonic regime is crossed. The transonic flight regime is especially critical as it is characterized by different, simultaneously occurring flow regions (subsonic/sonic/supersonic). However, the unsteady transonic variations are more crucial, as they often lead to markedly different aeroelastic behaviour depending upon the flow geometry (airfoil shape, angle-of-attack, control-surface deflections). The unsteady mixing of the different flow regions creates complex, time-dependent flow patterns, and causes interesting aeroelastic interactions. These include a significant dip in the flutter dynamic pressure, transonic buffet, LCO and control surface oscillation (buzz) caused by unsteady shock wave and boundary-layer interaction. Any of these phenomena can cause a catastrophic structural failure, if not properly addressed in airframe (open-loop) and active flight control (closed-loop) designs. In fact, these very transonic aeroelastic instabilities were historically dreaded as the 'sound barrier' which prevented safe supersonic flight in the first half of the 20th century. In the present age, nearly all airline transport aircraft fly in the high subsonic/transonic regime. Furthermore, fighter-type aircraft must not only cross the sonic speed but also perform high-g manoeuvres at transonic speeds in their mission. Hence, transonic ASE is even more important now than at any other time in the history of aviation.

Since transonic ASE applications involve unsteady shock motions, as well as periodic boundary-layer separation and reattachment induced by shock waves, advanced CFD modelling techniques are required for such inherently nonlinear effects (Silva *et al*. 2006). The inviscid, unsteady transonic equations required to capture shock waves are inherently nonlinear, even in their small-disturbance potential form. Furthermore, the presence of normal shock waves in the transonic flow exacerbates the transient (unsteady) flow behaviour by introducing nonlinear shock-induced flow oscillations, which can interact with the viscous boundary layer, thereby causing unsteady flow separation. The ASE plant for such a case is further complicated by the separated wake, or the leading-edge vortex from the wing interacting with the tail, resulting in irregular and often catastrophic deformation of the tail – either on its own or driven by a rapid and large deflections of the elevator. Such a wing–tail–elevator coupling of a post-stall buffet or a shock–vortex interaction requires a fully viscous flow modelling that is only possible by a Navier–Stokes method (Obayashi 1993). Another example of transonic ASE is the control of unsteady control-surface buzz and shock-induced buffet encountered by an aircraft manoeuvring in the transonic regime (Huttsell *et al*. 2001), leading to nonlinear flutter or LCO (Bendiksen 2004). An appropriate CFD model in such a case would require a FP, Euler or Navier–Stokes method, depending upon the geometry, structural stiffness, Mach number and Reynolds number. Sometimes, semi-empirical models are devised from wind-tunnel data for separated and shock-induced flows (Edwards 2008), because they do not require unsteady CFD computations to be performed in loop with structural dynamic and control-law calculations. However, the veracity of such a correlation must be checked carefully before being deployed in ASE design and analysis. An alternative method is to employ flight-test data for deriving an ASE model, such as the neural-network identification by Boëly and Botez (2010).

Any flow model that fully accounts for the unsteady transonic effects over an oscillating wing must necessarily be very complex, hence difficult to solve in real time. Owing to the inherent uncertainty of an unsteady aerodynamic model, a closed-loop controller for ASE

application must be quite robust to modelling errors. Furthermore, such a controller must also adapt to changing flight conditions, which renders it mathematically nonlinear even for a linear aeroelastic plant. This implies that as an accurate unsteady aerodynamics plant model is infeasible for aeroservoelastic design, adaptive plant identification in closed loop is the only practical alternative.

1.5 Adaptive Control Design

Following the above discussion, it is logical that the final step in aeroservoelastic system design should be the derivation of adaptive control laws that can fully account and compensate for the parametric uncertainties and variations in the characteristics of the aeroelastic system. Such control laws allow variation of the controller parameters in order to adapt to uncertain and changing plant characteristics. For this, an adaptation mechanism based upon the sensed (identified) input–output behaviour of the plant must be devised. Various adaptation mechanisms that can be applied to adaptive ASE design are now explored.

Design of a control system generally requires a plant model. The ability of a control system in achieving its desired performance depends upon how accurately the plant modelling is carried out. For example, the resolution of a digital camera depends upon how precisely the dynamics of the sensor, aperture and diaphragm are modelled. Similarly, the tolerance of a robotic positioning device largely depends upon the number of structural vibration modes considered in modelling the robotic arm. Most mechanical and electrical systems can be modelled to a very high accuracy because their dynamics are well understood, and hence controller design for the systems can be carried out by traditional methods. The same, however, cannot be said of an ASE system, wherein achieving high accuracy may result in the aeroelastic model becoming too unwieldy and complex to be of any benefit in control system design. For example, accurate modelling of a viscous, unsteady flow over a deforming wing surface would require unsteady, turbulent, Navier–Stokes solutions involving several thousands of grid points and hundreds of hours of computation time. The past several decades have seen significant advancement in CFD, but only at the cost of increasing complexity of modelling, which cannot be practical for closed-loop design and analysis. Rather than pursuing the course of increasingly accurate plant models, which seems to have reached a dead end, it is more profitable to look for simpler models that can capture the fundamental physical aspects of the aeroelastic plant. Therefore, accuracy is sacrificed in the interest of simplicity for a practical ASE design. Simplifying assumptions are usually made by neglecting some aspects of the plant characteristics, such as high-frequency dynamics, and structural and aerodynamic nonlinearities, thereby producing a mathematical model which is more amenable to control system design with either constant, or well-defined controller gains.

Consider an aircraft wing experiencing multimodal vibration in the presence of unsteady airloads. While in vacuo structural modelling of the wing can be accurately performed by a high-order finite-element method, the unsteady air loads acting on the wing are quite another matter. Depending upon the airspeed and altitude, the aerodynamic characteristics can range from low-subsonic, through transonic, to supersonic, each of which is dramatically and fundamentally different from the other. Furthermore, even in a given speed regime, a part of the flow on the wing could be laminar and another part turbulent, attached or separated, subsonic or supersonic, thereby creating almost infinite variation in the magnitude and phase of the dynamic loading. Since the structural deformations (elasticity) and air loads (flowfield)

are strongly coupled, each can cause a large change in the other at any given time, and this picture keeps on changing with time in an unpredictable manner. It can be said that an accurate aeroelastic model of the wing must take into account a large number of mutually coupled, randomly varying, local phenomena, an exact accounting of which is impossible. Even the most sophisticated aerodynamic model (Navier–Stokes equations with a statistical turbulence model) falls well short of faithfully capturing the complex flowfield around a flexing wing. Furthermore, such models are cumbersome in terms of computational efficiency, hence cannot be used in control system design. Therefore, the best available aeroelastic plant model is often an inaccurate and uncertain one.

How does one go about designing a good aeroservoelastic system if the plant is not well modelled? This question takes us to adaptive control design. A practical ASE system must operate at different design conditions representative of an aircraft flying at various speeds, altitudes and loadings. In many cases, the aerodynamic behaviour of the aircraft changes drastically when going from one flight regime to another, such as from subsonic to supersonic speeds. If not properly compensated for, the resulting aerodynamic changes (such as appearance of shock waves) can cause a large reduction in aeroelastic stability margin, perhaps leading to a catastrophic condition such as flutter. In order to maintain stability in the presence of varying flight conditions, one has two options: (i) meticulously redesign the control system at a large number of expected conditions and store the design points for a smooth interpolation of controller parameters in a given flight regime. This approach is called gain scheduling and is one of the first adaptive flight control strategies implemented in aircraft. (ii) Render the control system *self-adaptive* with respect to changing flight parameters through an extra feedback loop, which automatically compensates for loss of stability margin. While the former approach relies upon accurate plant modelling, the latter requires updating a 'workable' plant model by actual flight data in real time. Since it is only option (ii) that can be called adaptive in a true sense, it will be the main thrust of the present chapter. While most of the literature on ASE is concerned with accurate plant modelling by sophisticated structural and aerodynamic techniques that are necessary for the gain scheduling approach, we depart from this traditional approach and instead concentrate on developing good adaptive control algorithms that can achieve the closed-loop performance even in the face of a mathematically uncertain plant model. It can be appreciated by an aerodynamicist that even the best possible flow model may fail to capture many essential features of a flowfield, such as turbulent, separated and shock-dominated flows. Unfortunately, it is precisely such flow phenomena that are the most troublesome to an aeroservoelastician. Thus uncertainty in the plant model is unavoidable, and even becomes amplified as one approaches the transonic regime where the majority of modern aircraft operate. Furthermore, even if a high degree of modelling accuracy can been achieved at a particular design condition, the off-design operation usually becomes very sensitive to initial conditions and flow parameters, such as in the nonlinear buffet and limit cycle behaviour caused by separated flows. Owing to its inability to provide a reliable plant model across the flight regimes, the gain scheduling approach has proved to be inadequate for ASE purposes, and has not achieved flight certification status even more than 50 years after it was first devised. Clearly, the answer to a practical implementation of an ASE system lies in the alternative approach, namely self-adaptive control.

The ultimate example of self-adaptive control is the natural flight of birds, where a multitude of muscles move a group of feathers to produce a graceful flight. This is also a fine example of the juggling act involved in multivariable control, such as the symphony generated

by the concerted sounds of an orchestra. Such examples of nature provide a motivation and a challenge for the control engineer. Of course, it may be argued that the luxury provided by a plethora of natural control input variables – individually capable of modulation – is unavailable in the average engineering problem. This largely explains why the graceful, quiet and highly manoeuvrable trajectories of birds and insects are only in the realm of dreams of an aircraft designer. The control engineer has to work with a small number of control inputs, each of which is limited in magnitude and rate, often resulting in an underactuated plant. Thus the success in achieving a control objective relies solely upon the sophistication of the control laws employed for the purpose. The ASE designer is acutely aware of this limitation, and has to devote his energy in mathematically deriving a clever control strategy that could compensate for the deficiencies of his plant, which are both physical and mathematical.

1.5.1 Adaptive Control Laws

Adaptive control becomes necessary whenever the plant has either an unknown structure, unknown parameters or changing operating conditions, which imply an absence of any fixed description of input–output relationships. In such a case, an adaptive mechanism becomes necessary for the controller. For simplicity, we focus the discussion to state-feedback regulators, whose parameters are defined by the changing regulator gain matrix, $[K(t)]$. If an output-feedback scheme is used, the observer gains, $[L(t)]$, are also a part of the controller parameters. The adaptive controller is a self-adjusting system that can modify its parameters, $[K(t)]$, based upon the actual inputs, $\{u(t)\}$, applied to the plant, and the measurement of the actual outputs, $\{y(t)\}$, produced by the plant. In essence, an adaptive controller compensates for the lack of knowledge (or a change) of the plant's mathematical model by employing the measured plant characteristics. Owing to the dependence of the controller parameters on the plant's inputs and outputs, the adaptive controller is a nonlinear system, as depicted by the block diagram of Fig. 1.4. On comparison with the basic, fixed gain control system of Fig. 1.3, the presence of the additional adaptation mechanism is evident as the outer feedback loop, which allows for a change in controller parameters, $[K(t)]$, by a set of adaptation laws. Such a mapping of the plant's input and output vectors, $\{u(t)\}$, $\{y(t)\}$, onto the controller parameter vector space, $[K(t)]$, is the hallmark of an adaptive control system.

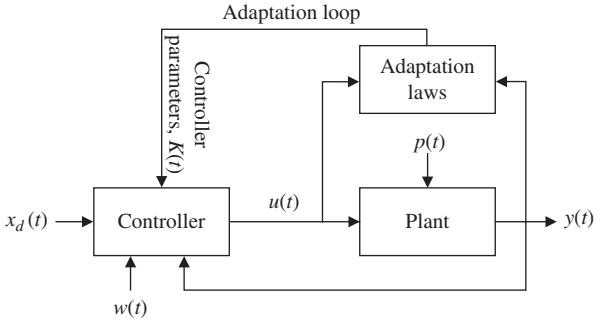

Figure 1.4 Generic adaptive control system with an adaptation mechanism for controller parameters

Adaptive control (Aström and Wittenmark 1995) arose as a discipline especially for designing the flight control systems of high-speed aircraft, which encounter large parametric variations in their operating envelope. Active research in the last several decades has produced many useful adaptive control techniques that can be applied to a wide range of problems. Unfortunately, these are specific to the application, rather than general, and can often be ad hoc procedures. The selection of an adaptive ASE control law is thus a challenging task, because an accurate aeroelastic model is unavailable in most cases. Hence, ASE has remained a formidable technological problem.

A part of the plant's output vector, $\{y(t)\}$, specifies the operating conditions. For example, a flight vehicle's operating (flight) conditions are the airspeed, altitude and Mach number. Often a good mathematical model of the plant can be derived for different sets of flight conditions (flight points), each having a set of linear controller parameters (gains) specially designed for it. In such a case, the adaptation mechanism is simply a table look-up of stored data points and the controller gains can be scheduled with the flight point. The resulting adaptive controller is called a gain scheduler. A schematic diagram of the gain schedule adaptation is shown in Fig. 1.5, where the inner feedback loop is the underlying linear control law for achieving stability for a given set of plant parameters, while the outer feedback loop determines the variation of the underlying controller parameters based upon a pre-set interpolation schedule. The gain scheduling approach was the earliest example of adaptive controllers designed for high-speed aircraft, rockets and spacecraft in the 1950s. As the name implies, most flight applications of gain scheduling involve an adjustment of linear feedback gains, but a more general application can also be envisaged where the controller parameters, $[K(t)]$, appear in a nonlinear relationship with the desired states, $\{x_d(t)\}$, and the outputs, $\{y(t)\}$, as shown in Fig. 1.5. Gain scheduling is thus regarded as a functional mapping method to vary the controller parameters $[K]$, $[L]$ according to the identified operating conditions. This requires solving for and storing the different sets of $[K]$, $[L]$ at various flight conditions. It can be expected that having to design controllers for a wide range of operating conditions requires a massive effort. Furthermore, as there is no possibility of taking into account either modelling errors or unmodelled (nonlinear) plant behaviour, gain scheduling is not regarded as an adaptive controller in the true sense.

A detailed and accurate model of the plant for various operating points is necessary before a gain scheduler can be designed for it, which is not always possible, especially for ASE plants in which we are presently interested. In a typical ASE application, the change in the plant's behaviour can be dramatic and not entirely predictable, such as in the case of transonic

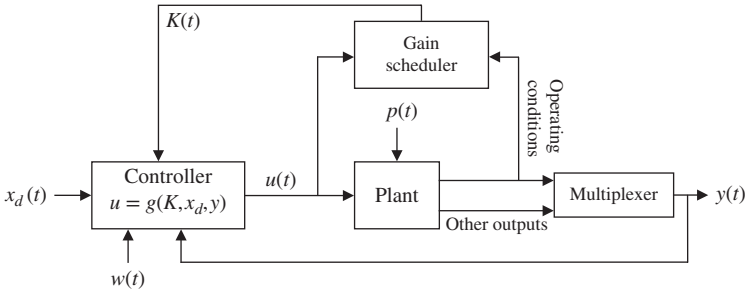

Figure 1.5 Schematic block diagram of a gain scheduling system

flutter and high angle-of-attack (stall) flutter. While an extensive research database exists on the transonic and high angle-of-attack flight, there are no efficient and reliable techniques available at present for modelling the essentially nonlinear characteristics of the aeroelastic plant under such conditions. In such a case, the gain-scheduling approach is not viable and recourse must be made to what is called a 'self-adaptive' control system.

Traditional self-adaptive systems for the regulation of an uncertain plant dynamics can be broadly classified into (i) self-tuning regulators (STRs) and (ii) model-reference adaptation systems (MRASs). An STR is an adaptive controller based on online parameter estimation of the unknown plant dynamics. A MRAS uses a predefined plant model (often linear and time-invariant) as its reference, in order to compare the actual behaviour, and to adapt the controller parameters accordingly. Since the desired behaviour is known a priori, such an adaptive mechanism is said to be *direct*. In contrast, an STR must first estimate the plant behaviour by sensing its input–output relationship in a closed loop and then apply an adaptation (or update) law for the controller parameters. Owing to the online identification of the plant's unknown behaviour, the self-tuning approach is called an *indirect* adaptation method. The two strategies can be further classified depending upon the types of adaptation laws and parameter identification algorithms they employ. We will consider STR for ASE systems in Chapter 5, while MRAS techniques will be the topic of Chapter 8.

A true adaptive controller must detect the actual plant behaviour, and apply a suitable correction to the underlying controller parameters in order to produce a stable closed-loop system. The most formal interpretation of this task is the STR whose schematic diagram is depicted in Fig. 1.6. Note the outer feedback loop for an online identification of the plant parameters, $[A]$, $[B]$, $[C]$, $[D]$, based upon a measurement of the plant's output vector, y, and a knowledge of the applied inputs, u. The slanted arrows in Fig. 1.6 indicate adaptation of the

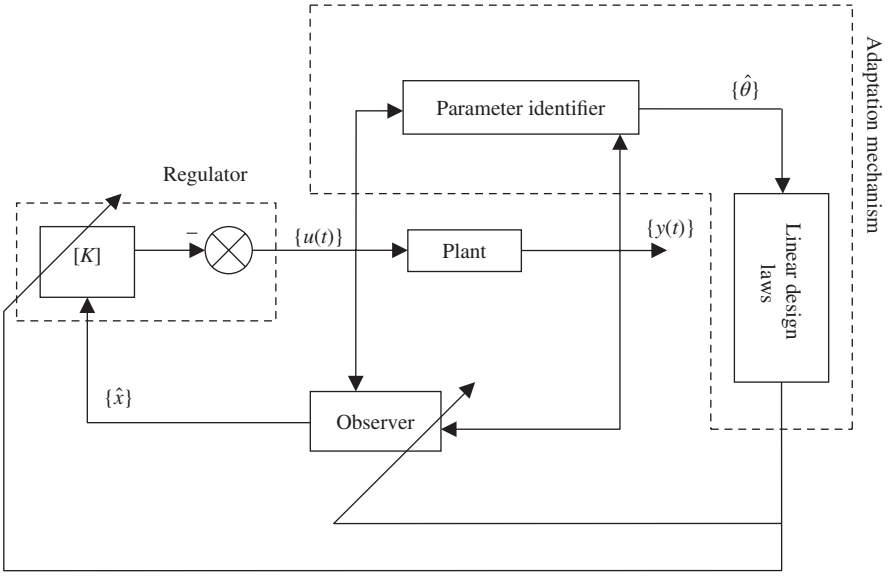

Figure 1.6 Schematic block diagram of a self-tuning regulator (STR)

parameters of the observer and the regulator. Consider a system with the following output equation:

$$\{y(t)\} = [\Phi(t)]\{\theta\}, \tag{1.26}$$

where $\{\theta\}$ are the unknown plant parameters arranged in a column vector and $[\Phi(t)]$ is a regressor matrix of functions of the known inputs and outputs. A parameter estimation scheme derives an estimate $\{\hat{\theta}\}$ by minimizing a positive cost function of the estimation error, $\{e\} = \{y\} - [\Phi(t)]\{\hat{\theta}\}$ at a given time t.

The parameter identification must be carried out with a finite record of the inputs and outputs. As the updated plant parameters become available, they are used to determine the new regulator and observer gains by solving the underlying linear control problem (such as the nonlinear AREs). The identification process is generally based on the solution to a set of linear algebraic equations, and hence the online controller updation is a much less complex task than that of accurately modelling the plant behaviour through a set of nonlinear partial differential equations. The success of the self-tuning approach depends upon active stabilization, rather than on how accurately the plant behaviour can be identified at any given instant. Therefore, guaranteeing closed-loop stability of the adaptation scheme is the primary objective. In some cases, it is even likely that a set of constant controller parameters are found to be stabilizing, albeit the plant parameters may be varying in time. The identified plant parameters are directly used in the underlying controller design, regardless of whether they are the 'true' parameters. Hence, the STR design approach is based upon the *certainty equivalence principle*, which disregards the uncertainty (or error) in plant identification.

The computation of the controller parameters from the underlying control design process of the STR can be transformed into a mapping from the plant's input–output record to the controller parameters space. The plant's parameter identification is then implicit in the adaptation mechanism, and it would appear that the controller parameters are being directly updated from the plant's input–output behaviour. An implicit dependence of the controller parameters on those of the identified plant is sometimes termed direct adaptation, whereas the explicit modules of identification and controller design in Fig. 1.6 is called indirect adaptation.

A variation of the direct STR is the MRAS, where the identification and controller design blocks are replaced by a reference model and an adaptation mechanism for the controller parameters, such that the error between the output of the reference model and that of the actual plant is minimized. Such a scheme is illustrated by the block diagram of Fig. 1.7. Note that when the reference input vector, $\{r(t)\}$, is removed from the MRAS, the result is very similar to the STR of the direct type. However, the methods of designing and implementing the MRAS and STR are quite different.

Consider a linear, time-invariant plant with a state-space model given by the following state-space equations with constant (but unknown) coefficient matrices $[A], [B], [C], [D]$, and unknown process noise, $\{p(t)\}$, and measurement noise, $\{m(t)\}$:

$$\{\dot{x}\} = [A]\{x\} + [B]\{u\} + \{p\}, \tag{1.27}$$

$$\{y\} = [C]\{x\} + [D]\{u\} + \{m\}. \tag{1.28}$$

If the plant's state vector, $\{x(t)\}$, can be directly measured, the following state-feedback law can be applied to stabilize the system:

$$\{u\} = -[K]\{x\} - [K_r]\{r\}, \tag{1.29}$$

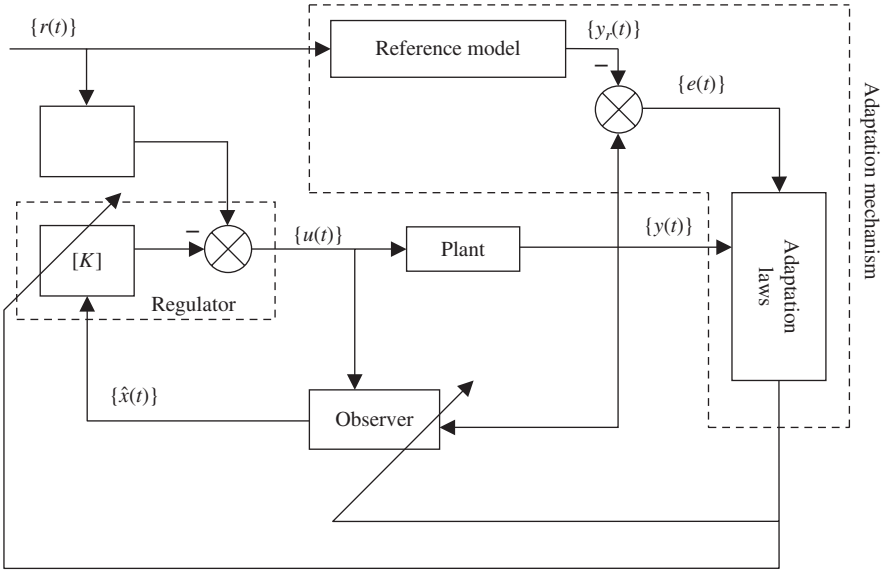

Figure 1.7 A model-reference adaptation system (MRAS)

such that the plant's state tracks a reference input vector, $\{r\}(t)$. Here $[K_r]$ is a feedforward gain matrix, and $[K]$ the regulator gain matrix. A reference model is defined by the following linear, time-invariant state-space representation with known coefficient matrices $[A_r], [B_r], [C_r], [D_r]$, and the reference input vector, $\{r(t)\}$:

$$\{\dot{x}_r\} = [A_r]\{x_r\} + [B_r]\{r\}, \tag{1.30}$$

$$\{y_r\} = [C_r]\{x_r\} + [D_r]\{r\}. \tag{1.31}$$

The estimated state, $\hat{x}$, required by the regulator is supplied by an observer (such as that given by Eq. (1.22)) whose gain matrix, $[L]$, must be designed on the basis of the plant's parameters, $[A], [B], [C], [D]$. Since the plant's parameters are uncertain, an exact set of stabilizing controller parameters, $[K], [K_r], [L]$, is unknown. Thus beginning from an initial guess of stabilizing controller gains, $[K(0)], [K_r(0)], [L(0)]$, the controller parameters must be evolved in time such that the error between the plant output and that of a reference model, $\{e\} = \{y(t)\} - \{y_r(t)\}$, is minimized in the limit $t \to \infty$. This is the broad philosophy behind MRAS schemes.

When the plant is inherently nonlinear, and cannot be linearized about an operating condition, a nonlinear feedback control-with an adaptation mechanism for its parameters – becomes necessary. A possible design strategy for such a controller is the geometric nonlinear feedback approach (Slotine 1995), such as adaptive feedback linearization, wherein the adaptive feedback renders the control system linear by cancelling its nonlinearities. However, a major shortcoming of feedback linearization is its inability to handle parametric uncertainties that are not matched by the control inputs (i.e., the uncertainties occurring in those state equations that do not contain the control inputs). Therefore, while the rigid body motion can be stabilized by adaptive feedback linearization, the same cannot be said for flexible structures or dynamic

aeroelastic systems. Furthermore, the cancellation of stable nonlinearities is undesirable, because it degrades the closed-loop response. Another popular geometric nonlinear method is the sliding mode (variable structure) control (Slotine 1995), which apart from the inability to stabilize unmatched uncertainties, is also unsuitable for aeroelastic applications because of the inherent problem of 'chattering' on the sliding surface. Consequently, adaptive feedback linearization, sliding mode control and other such geometric nonlinear feedback methods cannot be considered in an adaptive ASE design. There is very little mathematical treatment of nonlinear ASE effects in the literature. Traditional nonlinear ASE applications have employed frequency response aeroelastic models via describing functions. While such methods model structural nonlinearities (Dowell and I'lgamov 1988) by describing functions, they are not easily found for the nonlinear behaviour caused by separated and shock-dominated flows in the transonic regime. In addition, nonlinear adaptation ASE applications are absent in the literature. However, the describing function approach offers the promise of being used in conjunction with a recursive nonlinear identifier discussed below.

Alternatives to the nonlinear geometric feedback methods are the Lyapunov stabilization techniques of passivity-based methods (Haddad and Chellaboina 2008) and recursive back-stepping integration (Krstic *et al*. 1995). The advantage of the Lyapunov-based methods is that they can be easily applied to yield adaptation control laws required for MRASs and STRs. Unlike geometric control methods, the Lyapunov-based controllers do not depend very much on the plant characteristics, which offer a great flexibility in their design. This book mainly utilizes the Lyapunov-based methods for adaptive controller derivation. However, it is necessary to highlight the important theoretical concepts before applying them in the design process.

1.6 Organization

The treatment of all possible adaptive control techniques that could be applied to the design and analysis of ASE systems is a formidable task. This book attempts to do so by focussing on the important features and concepts. Chapter 2 details the feedback design methods applied to design the underlying controller, whose parameters are to be adjusted by a separate adaptation mechanism. Chapter 3 covers the basic principles and techniques used to derive an aeroelastic plant model that is suitable for use in controller design. Chapter 4 introduces the active suppression of the primary ASE instability, namely flutter, and presents examples of both typical-section (two-dimensional) and lifting-surface (three-dimensional) flutter. Chapter 5 introduces STRs for adaptive ASE systems based upon online plant identification. Chapter 6 details the essential concepts used in analysing the stability, and designing stabilizing controllers for nonlinear systems, of which adaptive ASE systems are the target. Chapter 7 presents the methodology of describing functions analysis, and Nyquist-like techniques based upon Circle and Popov criteria, which can be applied to model LCOs associated with nonlinear aeroelastic behaviour caused by shock-induced and separated flows. Chapter 8 focuses on MRAS techniques, with applications to ASE systems. Chapter 9 presents the essentials of the powerful adaptive control method via backstepping integration as an alternative to the traditional methods (MRAS and STR). Chapter 10 considers robust design of adaptive systems in the presence of nonlinearities and noise inputs. Finally, Chapter 11 covers the ultimate end of adaptive ASE design, namely the possible handling of transonic flutter and LCOs by adaptive control methods.

References

Abel I 1979 An analytical design technique for predicting the characteristics of a flexible wing equipped with an active flutter suppression system and comparison with wind-tunnel data. *NASA Technical Publication* **TP-1367**.

Abel I and Noll TE 1988 Research and applications in aeroservoelasticity at NASA Langley Research Center. *Proceedings of the 16th ICAS Congress*, Tel Aviv, Israel.

Aström KJ and Wittenmark B 1995 *Adaptive Control*. 2nd ed., Addison-Wesley, New York.

Bendiksen OO 2004 Transonic limit-cycle flutter/LCO. *AIAA Paper* **2004-2694**.

Boëly N and Botez RM 2010 New methodologies for the identification and validation of a nonlinear F/A-18 model by use of neural networks. *Proceedings AIAA Atmospheric Flight Mechanics Conference*, Toronto, Canada.

Dowell EH and I'lgamov M 1988 *Studies in Nonlinear Aeroelasticity*. Springer-Verlag, New York.

Edwards JW 2008 Calculated viscous and scale effects on transonic aeroelasticity. *J. Aircr.* **45**, 1863–1871.

Glover K and Doyle JC 1988 State space formulae for all stabilizing controllers that satisfy an H_∞ norm bound and relations to risk sensitivity. *Syst. Control Lett.* **11**, 167–172.

Haddad WM and Chellaboina V 2008 *Nonlinear Dynamical Systems and Control*. Princeton University Press, Princeton, NJ.

Huttsell L, Shuster D, Vol J, Giesing J, and Love M 2001 Evaluation of computational codes for loads and flutter. *AIAA Paper* **2001-569**.

Krstiè M, Kanellakopoulos I, and Kokotoviè PV 1995 *Nonlinear and Adaptive Control Design*. Wiley-Interscience, New York.

Maciejowski JM 1989 *Multivariable Feedback Design*. Addison-Wesley, Reading, MA.

Obayashi S 1993 Algorithm and code development for unsteady three-dimensional Navier-Stokes equations. *NASA Contractor Report* **CR-192760**.

Packard A and Doyle JC 1992 A complex structured singular value. *Automatica* **29**, 71–109.

Perry B, Cole S, and Miller GD 1995 A summary of the active flexible wing program. *J. Aircr.* **32**, 10–15.

Silva WA, Mello OAF, and Azevedo JLF 2006 Sensitivity study of downwash weighting methods for transonic aeroelastic stability analysis. *J. Aircr.* **43**, 1506–1515.

Slotine JJE and Li W 1995 *Applied Nonlinear Control*. Prentice-Hall, Englewood Cliffs, NJ.

Tewari A 2002 *Modern Control Design with MATLAB and Simulink*. John Wiley & Sons, Ltd, Chichester.